Hydrological Processes

WILEY

RESEARCH ARTICLE OPEN ACCESS

Storage Dynamics and Groundwater–Surface Water Interactions in a Drought Sensitive Lowland Catchment: Process-Based Modelling as a Learning Tool

Zhengtao Ying[1,2] | Doerthe Tetzlaff[1,2,3] | Jean-Christophe Comte[3] | Songjun Wu[1,2] | Chris Soulsby[1,3,4]

[1]Leibniz-Institute of Freshwater Ecology and Inland Fisheries, Berlin, Germany | [2]Geography Institute, Humboldt University of Berlin, Berlin, Germany | [3]Northern Rivers Institute, School of Geosciences, University of Aberdeen, Aberdeen, UK | [4]Department of Forest Ecology and Management, Swedish University of Agricultural Science (SLU), Umeå, Sweden

Correspondence: Zhengtao Ying (zhengtao.ying@igb-berlin.de)

Received: 13 January 2025 | **Revised:** 27 March 2025 | **Accepted:** 15 April 2025

Funding: This work was supported by China Scholarship Council; Wallenberg Foundation (WP2023-0001); Einstein Foundation Berlin (ERU-2020-609).

Keywords: drought | groundwater modelling | particle tracking | storage change | water budgets

ABSTRACT

Groundwater is a key strategic water resource in times of drought, yet climate and land use change are increasing threats; this means that quantitative understanding of groundwater dynamics in lowland catchments is becoming more urgent. Here, we used a spatially distributed numerical groundwater model to simulate seasonal and long-term changes in the spatio-temporal patterns of water storage dynamics and groundwater–surface water interactions in the 66 km^2 lowland Demnitzer Millcreek catchment (DMC) in NE Germany. DMC experienced a long period of drought following the hot, dry summer of 2018, with groundwater stores becoming depleted and stream flows increasingly intermittent. The architecture and parameterisation of the model domain were based on groundwater observations, hydrogeological mapping and geophysical surveys. Weekly simulations using a single model layer with a 50 × 50 m grid of 15 m depth were able to broadly reproduce observed shallow groundwater dynamics in glacial and post-glacial deposits across the catchment. We showed that most groundwater flow is shallow and focused around topographic convergence zones fringing the channel network in more permeable glaciofluvial deposits. Most stream flow is generated by shallow groundwater in the catchment headwaters, which is relatively young (i.e., ~5 years old). With potential evapotranspiration rates exceeding precipitation, the groundwater balance is very sensitive to hydroclimate at DMC. The past two decades have been dominated by negative anomalies in annual rainfall, causing a general lowering of water tables and persistent storage deficits. Spatio-temporal patterns of recharge are also strongly influenced by vegetation cover, with coniferous forests, in particular, having high evapotranspiration losses that inhibit groundwater recharge. This underlines the importance of developing integrated land and water management strategies in NE Germany where climate change is expected to further reduce rainfall, increase temperatures and decrease groundwater recharge. For an evidence base to guide policy, we need to develop more robust ways to interface groundwater models with ecohydrological models to better characterise the impacts of land use on rechange in groundwater-dominated lowland catchments.

1 | Introduction

Groundwater is the major freshwater store in the hydrological cycle and plays a crucial role in meeting human and ecological water needs in lowland areas (Döll et al. 2012). Groundwater not only supports irrigated agriculture and urban water supply across much of the world but also dominates the base flow of rivers, especially in areas with shallow aquifers where groundwater readily exchanges with surface water (Soulsby et al. 2015; Winter 1999). However, shallow aquifers often have limited water storage capacity and are more directly susceptible to human activities such as abstraction and pollution sources; they also are sensitive to hydroclimatic variability and climate change (Condon et al. 2020; Kløve et al. 2014; Santos et al. 2014). Recent increases in the frequency and intensity of drought in many regions reflect the impacts of climate change (Peterson et al. 2021; Yuan et al. 2023) and, in some areas, have significantly reduced groundwater recharge, which, together with increased groundwater use as a more consistent source of water supplies, has promoted alarming decreases in water table levels (Jasechko et al. 2024; Oiro et al. 2020; Taylor et al. 2013). In shallow aquifers, this can have far-reaching implications for groundwater–surface water interactions that are closely linked to recharge and storage changes, and thus threatens the maintenance of river flows and wetlands (Kleine, Tetzlaff, Smith, Goldhammer, et al. 2021). These changes have made regional water management in drought-sensitive areas more complex and urgent; further increasing the strategic importance of groundwater. Although global trends in groundwater storage are available from GRACE satellite products (Richey et al. 2015), the coarse resolution means that these data are often of limited assistance for assessing local change and developing management responses. For local and regional scales, improved quantification of the three-dimensional water storage continuum in the subsurface of intermediate-sized catchments is a useful pathway to enhancing both ecohydrological and societal resilience to droughts (Tetzlaff et al. 2024). In such situations, quantitative, process-based understanding of the dynamics of groundwater recharge and depletion, together with characterising the spatio-temporal patterns of groundwater and surface water interactions, is particularly critical.

In order to characterise and quantify spatial and temporal patterns of water storage and flow in groundwater systems, numerical modelling is an important approach. MODFLOW (Harbaugh 2005) is one of the most commonly used groundwater models and has simple connected surface water modules in the form of boundary conditions, such as rivers, streams and lakes. A number of groundwater–surface water models have been developed that use it as the groundwater module. For example, SWATMOD couples the widely applied Soil Water Assessment Tool (SWAT) model with MODFLOW; GSFLOW combines the Precipitation Runoff Modelling System (PRMS); and MODHMS introduces 2-D diffusion wave routing for surface water into MODFLOW (Ntona et al. 2022). A trend in new models is the full coupling of the shallow flow equations with the Richards equation for linked groundwater and surface water simulations (e.g., ParFlow and HydroGeoSphere) (Ma et al. 2024). These models have been applied at scales from small catchments (Ala-aho et al. 2017) to large managed watershed and regional groundwater flow systems (Bianchi et al. 2024; Panagopoulos 2012; Reeve et al. 2001) and successfully helped resolve different water resources issues, including the effects of climate change on groundwater storage (Goderniaux et al. 2009; Saha et al. 2017; Zipper et al. 2021), irrigation and pumping impacts (Dehghanipour et al. 2019; Tian et al. 2015) and water exchange between rivers and aquifers (Devia et al. 2015; Frei et al. 2009; Yang et al. 2025). However, the accuracy and robustness of models can be aided by using direct observational data in calibration and/or validation (Anderson et al. 2015), making application at data-rich sites particularly valuable.

The North German Plain is an extensive lowland region that has recently been experiencing the consequences of climate change, with five consecutive years of negative rainfall anomalies between 2018 and 2022 (Imbery et al. 2023). Resulting reductions of crop yields, depletion of aquifers and increased intermittency of stream flows have increased the need for an improved scientific evidence base to guide sustainable approaches to land and water management. The Demnitzer Millcreek catchment (DMC) in northeastern Germany is a long-term environmental observatory, which has been operating since 1980. Research initially centred on understanding agricultural water pollution (Gelbrecht et al. 2005), but more recently has focused on ecohydrology and land use implications for water security (Tetzlaff et al. 2022). Research has shown that runoff from the catchment is mainly sustained by shallow groundwater in a range of glacial, glaciofluvial and post-glacial alluvial deposits, with seasonal stream flow variations showing strong correlation with riparian water table levels (Kleine, Tetzlaff, Smith, Dubbert, et al. 2021). Moreover, the catchment has a complex cover of mixed land use, ranging from croplands to forests, with contrasting evapotranspiration losses leading to spatially variable patterns of groundwater recharge, which can be 50% lower under forests (Luo et al. 2024a; Smith et al. 2021, 2022). The persistent drought since 2018 has resulted in rivers within the catchment and wider region being characterised by increasingly intermittent flows restricted to the winter (Wang et al. 2025). This has been related to the drought resulting in substantial declines in recharge and storage, with weaker groundwater–surface water interactions (Luo et al. 2024b).

Building on long-term data collection at DMC, groundwater investigations have expanded since the 2018 drought. A conceptual model of groundwater–surface water interactions has been developed using basic data obtained from multi-proxy approaches integrating water table monitoring, hydrogeophysics and tracer studies (Ying et al. 2024). The objective of the current study was to extend this previous work and develop a preliminary, quantitative groundwater model for the catchment in order to assess storage dynamics and groundwater–surface water interactions. Using the process-based modelling as a learning framework, the specific research questions were:

1. What are the effects of hydroclimate on the water balance and groundwater dynamics?
2. How do physiographic features and land use affect spatial–temporal patterns of groundwater–surface water interactions?
3. What are the spatio-temporal dynamics of groundwater vulnerability to drought and implications for recovery?

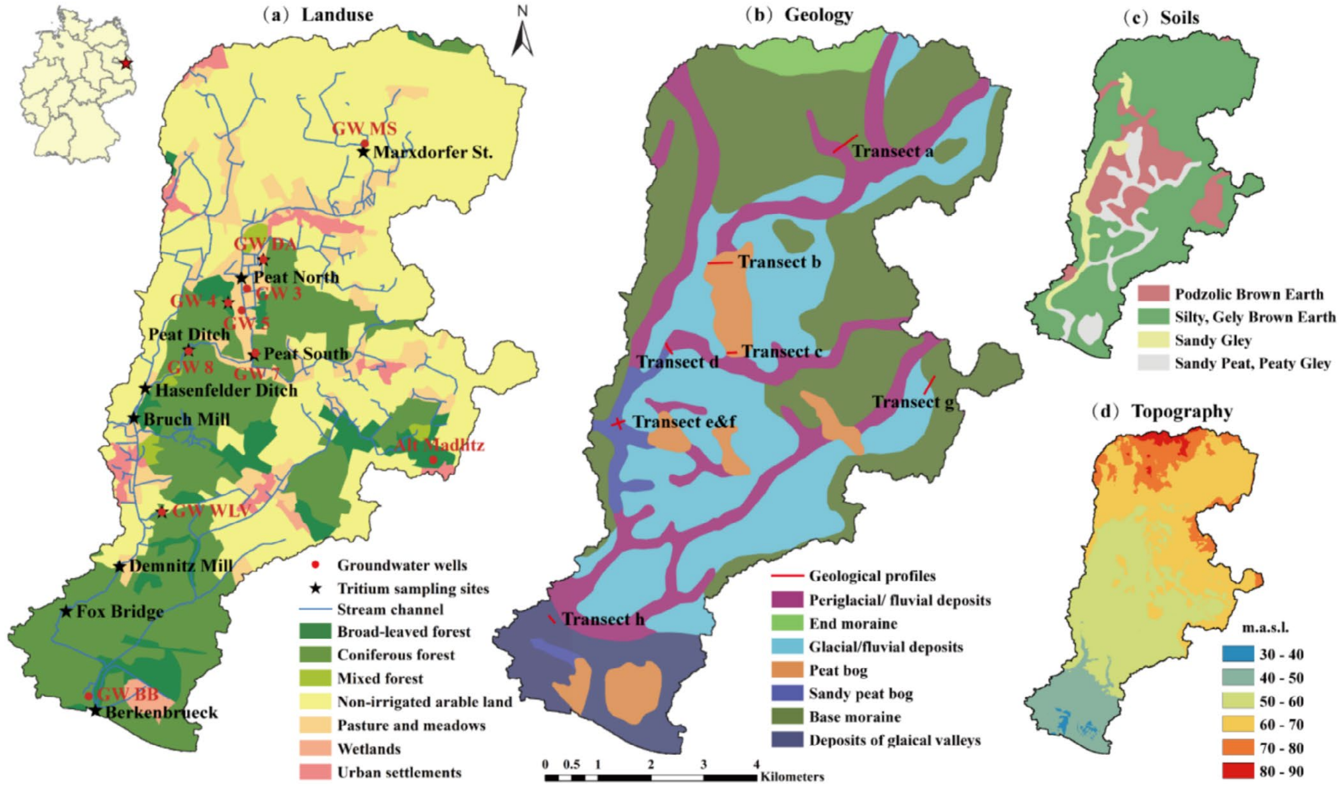

FIGURE 1 | Location of the study area in Germany (red star). (a) Land use map of the Demnitzer Millcreek catchment and locations of tritium sampling and groundwater wells, (b) catchment geology and geological profiles, (c) surficial soils and (d) surface elevation above mean sea level (m).

2 | Study Site and Data

The study site at DMC (52°23′ N, 14°15′ E) is a 66 km^2 lowland catchment located in the NE of Germany, 55 km east of Berlin (Figure 1). The catchment is relatively flat, with elevation ranging from 38 to 88 m.a.s.l. and an average slope of < 2% (Figure 1d). DMC has a typical humid continental climate with warm summers and cool winters (Kottek et al. 2006) (Figure 2a). Long-term mean air temperature (since 2001) is 9.7°C, and cumulative annual precipitation varies from 376 to 792 mm. Precipitation in winter is largely associated with low-intensity frontal rain, whilst larger intense convectional events characterise the slightly wetter summer period. Annual potential evapotranspiration (PET) is high relative to the annual precipitation and ranges from 650 to 700 mm (UFZ, 2020).

Land use is currently dominated by agriculture, with more than 60% of the area covered by non-irrigated arable crops or grasslands, particularly concentrated in the upper regions (Figure 1a). Forestry, mainly coniferous plantations of Scots Pine (*Pinus sylvestris*) is the second major land use and increases in importance downstream, accounting for 36% of the area. Some small urban settlements are distributed in DMC, but the overall population is low (~5000 residents).

Shallow exploration boreholes (Figure S1) and hydrogeophysical surveys (Ying et al. 2024) showed that the local hydrogeology is controlled by extensive accumulations of superficial glacial and post-glacial sediments (Figure 1b). The catchment is underlain by glacial, glaciofluvial and alluvial deposits. Clay-rich basal and end moraines with relatively low permeability outcrop in the elevated interfluves in the east, north and west of the catchment. Elsewhere, particularly along the river channel network, the poorly productive moraines are overlain by more permeable glacial, periglacial and modern fluvial-alluvial deposits forming a more productive shallow aquifer system, which becomes thicker towards the outlet of the catchment in the south, characterised by the presence of an incised glacial valley (Figure 1b). Glaciofluvial and fluvial/periglacial deposits have the highest hydraulic conductivity and storativity, permitting significant groundwater flow and storage (Ying et al. 2024).

The catchment is characterised by four major soil types, which closely relate to the distribution of glacial drift deposits (Figure 1c). The dominant soils are silty brown earths, which cover 72.1% of the catchment and are found on the imperfectly drained basal moraine deposits (Figure 1c). The better arable farming is found on these more water-retentive soils, whilst forestry areas dominate on the more free-draining sandy brown soils overlying glacial/fluvial deposits. Gleyed soils fringe the river valleys, though in some low-lying areas, peat deposits have formed in the post-glacial, creating wetland areas. Grassland and grazing are the dominant land uses on the peats and gleyed soils.

Groundwater in DMC is shallow, with the water table typically within 3 m of the ground surface, and < 1 m in the wetlands (Figure 2c). The annual depth range usually varies by ~0.5–1 m, with late winter/early spring maxima and late summer/autumn minima. Streamflow is closely correlated with groundwater levels and ceases in most summers as groundwater levels fall below the riverbed, commencing again in autumn as the water table rises.

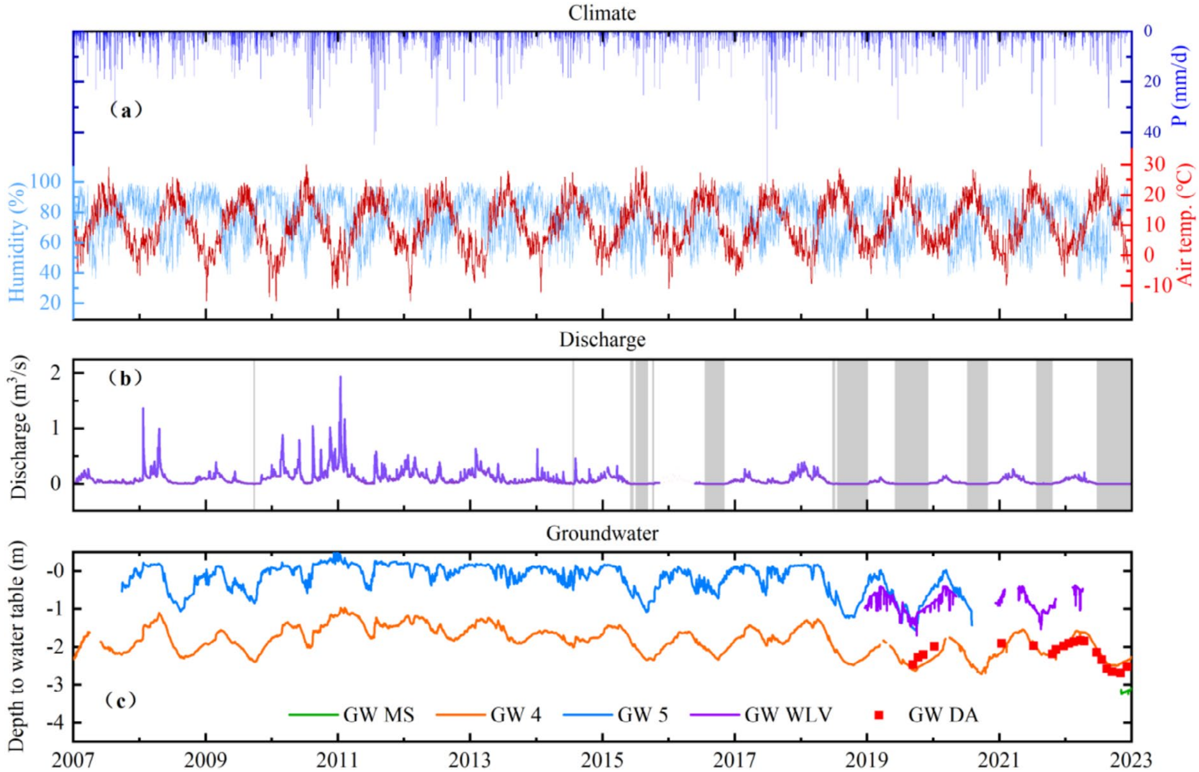

FIGURE 2 | Timeseries of DWD (German weather service) data of precipitation, relative humidity and air temperature (a), daily discharge from the location Demnitz Mill, with grey areas indicating no flow (b), long-term daily groundwater levels (c).

3 | Modelling Framework

3.1 | Groundwater Model Setup and Discretisation

We used the USGS MODFLOW-2005 code for groundwater modelling in DMC, compiled within the open-source Python framework FloPy (Bakker et al. 2016). Geophysical investigations and exploration piezometers showed that much of the shallow-circulating groundwater in the catchment was stored in moderately permeable periglacial colluvium, as well as fluvial and sandy peat deposits in riparian areas. These overlay the low-permeability clay-dominated basal moraines, with the moraine being generally 10–15 m below the ground surface where it is not outcropping (Ying et al. 2024). Consequently, we chose to set up a simplified one-layer model with a thickness of 15 m and divided the model into different geological units based on the geological maps, shallow boreholes and ERT data from previous work by Ying et al. (2024). Each grid cell was assigned the hydrogeological properties of the mapped unit. The model area of 66 km^2 was represented by a finite-difference grid of 200 rows and 273 columns with a uniform grid cell size of 50 m to allow small surface water features to be included in the model (Figure 3). A DEM from 2019 was used as the upper model elevation with a resolution of 10 m.

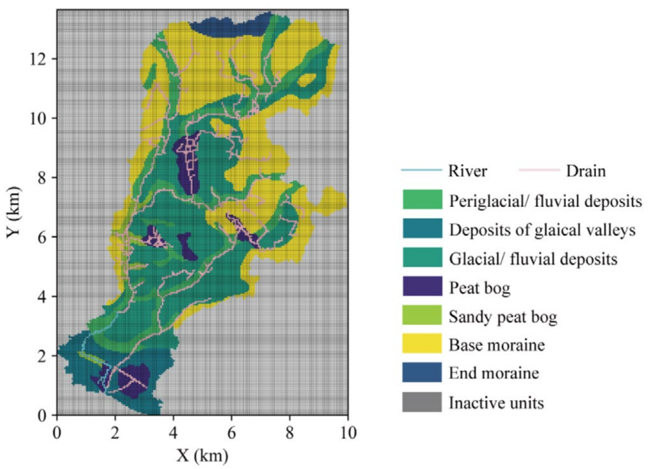

FIGURE 3 | Plan view of the DMC catchment showing the hydrogeology model and boundary conditions, and grey areas indicate inactive units.

3.2 | Parameterisation

Each geological unit was parameterised by values for horizontal hydraulic conductivity, specific storage, specific yield, vertical anisotropy and porosity and distributed according to the geological mapping. The vertical anisotropy was set to 1, and porosities were set from 0.15 to 0.80 for different hydrogeological units (Fetter 2018). Initial parameter ranges, based on local field information where available, and literature values where not, are shown in Table 1 (Adamo et al. 2021; Freeze and Cherry 1979). These ranges primarily differentiated the low permeability base and end moraines from the more permeable glaciofluvial and alluvial deposits.

TABLE 1 | Model parameters and ranges for calibration, values referenced from Freeze and Cherry 1979; Fetter (2018) and Adamo et al. (2021).

Name	Hydraulic conductivity Kh (m/s)	Specific yield Sy (–)	Specific storage Ss (m^{-1})	Conductance Cd (m^2/day)
Peat bog	1^{-8}–1^{-2}	0.10–0.45	10^{-5}–10^{-3}	—
End moraine	1^{-12}–1^{-5}	0.10–0.30	10^{-5}–10^{-3}	—
Deposits of glacial valleys	1^{-5}–1	0.10–0.30	10^{-5}–10^{-3}	—
Glacial/fluvial deposits	1^{-5}–1	0.10–0.30	10^{-5}–10^{-3}	—
Periglacial/fluvial deposits	1^{-8}–1^{-4}	0.10–0.30	10^{-5}–10^{-3}	—
Sandy peat	1^{-6}–1^{-2}	0.10–0.45	10^{-5}–10^{-3}	—
Base moraine	1^{-8}–1^{-4}	0.10–0.30	10^{-5}–10^{-3}	—
Drain	—	—	—	10–1000

3.3 | Boundary Conditions

In order to simplify the model, we set all lateral and lower (base moraine clays) boundaries of the model domain as no-flow boundaries. It was recognised that this would introduce uncertainties regarding potential lateral subsurface flow out of, or into, the flat catchment area and possible deeper seepage. However, in the absence of more detailed information, this was deemed suitable for a first approximation of the groundwater flow system, given the low flow/storage properties of the basal moraines.

Applied weekly recharge to MODFLOW across the domain of the catchment groundwater model was computed using four land use-related implementations of the LUMPREM model (Doherty 2020) to account for unsaturated zone evapotranspiration losses. These areas are depicted in Figure S2 and comprise four land uses (agriculture, forest, grass and urban). LUMPREM operates on a daily time step. It takes daily values of rainfall and potential evaporation from weather stations as input. From this, cumulative weekly estimates of recharge were applied to the top layer of MODFLOW cells, which were dependent on rainfall inputs, evapotranspiration outputs and the capacity of the soil-moisture store. LUMPREM takes potential evapotranspiration as a sequence of daily inputs. However, the rate at which plants actually evapotranspire is dependent on the volume of water within the soil moisture store and the effects on stomatal conductance for different vegetation. The rate of water loss through evapotranspiration is calculated using the equation:

$$E = fE_p \frac{1 - e^{-\gamma v'}}{1 - 2e^{-\gamma} + e^{-\gamma v'}} \tag{1}$$

where E_p is potential evaporation; f can be considered as a crop factor (agriculture: 0.8, forest: 0.85, grass: 0.7 and urban: 0.4); v' is the relative volume of water in the soil moisture store and γ is a fitting parameter.

In addition, the MODFLOW evapotranspiration package (EVT) was applied to simulate any additional effects of plant transpiration uptake or direct evaporation from the saturated zone (McDonald 1988). These losses all draw from the topmost active cell and we set the extinction depth to 3 m. The EVT package also operates with different parameterisations for each of the four land uses, and potential evapotranspiration calculated by LUMPREM provides the maximum ET input for the EVT package.

The drain package (DRN) was applied to simulate the groundwater inflow into the stream network, where the depth of the drain (drain elevation) was set to 2, 0.5 and 1.5 m from upstream to downstream depending on field-measured values, and a conductance value was adjusted during model calibration. When the head in the aquifer is above the drain elevation, the groundwater discharges to the drain at a rate proportional to the difference in head. If the aquifer head falls below the drain elevation, then the drain has no effect on the aquifer. The rest of the cells also have the drain module set, but at a depth of 0 m in order to prevent the groundwater level from being higher than the surface, particularly in riparian wetland areas.

The river package (RIV) was only set in the channel section below Demnitz Mill (Figure 3). On the one hand, this setup ensured a water level base for the model. On the other hand, the downstream is affected by a larger aquifer, and the river is permanent at the outlet. We simplified this to a rectangular river network, and the conductance can be computed as

$$\mathrm{CRIV}_n = \frac{K_n L_n W_n}{M_n} \tag{2}$$

where K_n is the hydraulic conductivity of the riverbed material, we set 1 m/d; L_n represents the length of the river as it crosses the node, 50 m; W_n is the river width; and M_n is the thickness of the riverbed layer. We set the river width to 1.5 m and the thickness of the riverbed to 1 m based on average observed values.

3.4 | Observational Data and Calibration

The observational hydrometric data to aid groundwater modelling in DMC comprise hydraulic head and stream discharge. Hydraulic head observations were available for a network of sites (Ying et al. 2024), with 3 distributed observation wells being used for calibration (GW MS, GW 4 and GW WLV). (Figure 1). Gauging stations located at Peat North (PN), Peart South (PS), Bruch Mill (BM) and the catchment outlet at Demnitz Mill (DM) measured stream discharge. The daily average discharge for the period 2001–2022 was 0.1 m^3/s though this varies with climate (Figure 2b). Water table elevations in other wells (GW3, GW5 GWDA), stream discharge at PN and BM, along with tritium-derived water age estimates in groundwater and stream water, were used as "soft" data to evaluate the model results. In addition, a well installed at Allt Madlitz in 2023 provided a qualitative indication of groundwater levels in the west of the catchment, even though this did not coincide with the modelling period.

Parameters were Latin hypercubic sampled according to the ranges in Table 1 and transformed to a uniform distribution. Monte Carlo simulations were performed on the resulting set of 100000 parameters. R^2 and RMSE were calculated separately for each groundwater well, and weights were configured according to the number of samples.

3.5 | Groundwater Budgets

The groundwater budgets were obtained from the MODFLOW listing file (Harbaugh 2005), and the zone budget of four land uses was extracted from the cell-by-cell flow file. Then the total groundwater budget equation can be defined as follows:

$$\sum_{i=i}^{n} Q_{\mathrm{IN},i} - \sum_{i=i}^{m} Q_{\mathrm{OUT},i} = \Delta S \quad (3)$$

where $\triangle S$ is storage change, L^3/T. Q_{IN} means inflow components, including applied recharge into the model domain from precipitation ("recharge"), contribution to groundwater from rivers ("rivers recharge"). Q_{OUT} is groundwater outflow, including groundwater discharge to rivers ("rivers discharge"), groundwater discharge to drains ("drains discharge") and loss from evapotranspiration ("ET loss") from the EVT package. In groundwater modelling, storage release (to meet water balance demands) is typically considered an inflow component, whereas storage intake (to replenish depleted aquifer storage) is considered an outflow component, although no actual transfer of water into or out of the groundwater system occurs with either of these processes (Anderson et al. 2015). A positive $\triangle S$ indicates water surplus and a corresponding rise in groundwater levels. Conversely, groundwater decreases with water deficit.

3.6 | Particle Tracking

Based on the flow field computed by the calibrated groundwater model described above, a simple particle tracking analysis was performed using MODPATH7 to give a first approximation of the groundwater flow pathways. The results of this program represent the groundwater travel times and flow paths for advective transport only. To estimate the tracking times, an effective porosity value was defined for each cell in the grid. We set the same porosity for the same geological unit according to a reference range (Fetter 2018), which is shown in Table S1. Forward and backward particle tracking was performed using MODPATH. A set of particle-starting locations that surround the cell containing the groundwater wells was specified, along with random points throughout the catchment. Particles were tracked forward to track dynamics that infiltrated water from the surface into the shallow aquifer and backward from the groundwater wells to locate the origin of the flow paths.

4 | Results

4.1 | Groundwater Levels

The model was driven at weekly time steps using the available hydroclimatic data, with losses estimated by using the LUMPREM, RCH and EVT packages (see annual summaries in Table 2). Net recharge to groundwater after accounting for these losses varied between 376 mm in the wet year of 2010 and just 1 mm in the drought year of 2018.

The model could reproduce the general differences in groundwater levels across the catchment (Figure 4). As an example, the free draining forested areas in the central catchment were simulated reasonably well at GW4, though recharge seemed underestimated in dry years, resulting in underprediction of summer peaks (see time series in Figure S3). Other calibration wells in the upper catchment at GWMS and lower catchment (GWWLV) were also reproduced quite well, along with the deeper groundwater levels at GWDA. Additionally, uncalibrated shallow water table dynamics in the peatland (GW3 and GW5) were captured, though as the modelled levels did not allow for standing water (which was present in some winter wet-periods), systematic underprediction is evident. Further, it was reassuring that an area where deeper water table levels were simulated (5–10 m deep) at Allt Madlitz in the east of DMC was consistent with deeper levels recently at a new monitoring well that was installed in 2023, so not used in the modelling.

At the catchment scale, simulated groundwater elevations showed flow directions from north to south with decreasing water elevations. (Figure 5a). The generally shallow water table was reproduced with variations in the depth to water table primarily reflecting topography, and the water table was around 10 m deep in the northern and western catchment where the topography is higher, and less than 1 m deep in the wetlands and riparian areas (Figure 5b). This general flow system was consistent through the simulation period, with only local groundwater flow patterns, particularly close to the stream network, changing in response to wetter and drier periods. In wet years, the greatest increase in groundwater levels was in the forested areas in the mid- and lower parts of the catchment (~0.3 m) (Figure 5c). Across the rest of the model domain, the increase was between 0.1 and 0.3 m. In dry years, the decline in groundwater is greater in the southern region, particularly in deposits of glacial valleys (Figure 5d). The counter-intuitive increase in groundwater in the upper catchment in 2018 reflects the effects of a wet winter in 2017/early 2018 and the greater recharge in non-forest areas. As shown below, these spatial patterns of storage change in relation to hydroclimatic variations reflected the integrated effect of the differences in storage capacity in contrasting sediments and the associated effects of land cover on evapotranspiration. These spatio-temporal changes in groundwater elevations and depth to the water table were shown in more detail in the animations shown for the entire simulation periods in Figures S4 and S5.

TABLE 2 | Annual data (mm).

Year name	2007	2008	2009	2010	2011	2012	2013	2014	2015	2016	2017	2018	2019	2020	2021	2022
Precipitation[a]	691.0	596.8	580.5	791.8	572.1	622.4	611.2	474.2	495.9	495.4	739.4	397.7	520.3	510.5	536.3	500.7
Discharge[a]	25.9	56.2	33.9	108.5	90.4	63.4	54.8	29.0	24.9	5.7	33.5	31.9	6.9	11.5	25.2	15.6
PET[a]	745.3	731.8	737.4	699.4	769.0	735.8	687.1	719.3	802.3	748.8	714.1	883.5	841.1	799.3	742.5	854.1
Recharge[b]	492.1	395	356.3	571.5	401.7	400.7	422.5	286.2	288.3	289	517.6	205.4	295.4	315.7	318.2	287.9
ET[b]	221.2	200.7	204.1	195.2	206.3	210.6	200.3	194.0	203.7	196.8	217.7	204.6	220.0	210.9	196.9	212.8
Storage change GW4[c]	133.5	−18.9	39.1	170.3	−42.4	−49.7	−47.3	−11.7	−66.9	24.0	102.1	−226.2	−18.0	34.9	61.8	−91.3
Storage change GW5[c]	298.5	−55.7	98.2	97.5	−17.5	−11.6	−16.0	0.7	−86.1	74.0	16.23	−150.3	−22.8			
Storage change GW8[c]	162.7	−21.3	6.3	57.6	−67.7	−6.5	41.2	−26.7	−44.5	−2.3	79.2	−187.0	−32.4	46.5	68.7	−118.3
Storage change GW WLV[c]													22.3	−2.2	33.7	−62.8

[a]Data are from actual measurement.
[b]Data are from LUMPREM output, including groundwater recharge and evapotranspiration.
[c]Groundwater storage change (GW4/5/8/WLV) is obtained by multiplying the change in measured water level by the specified yield.

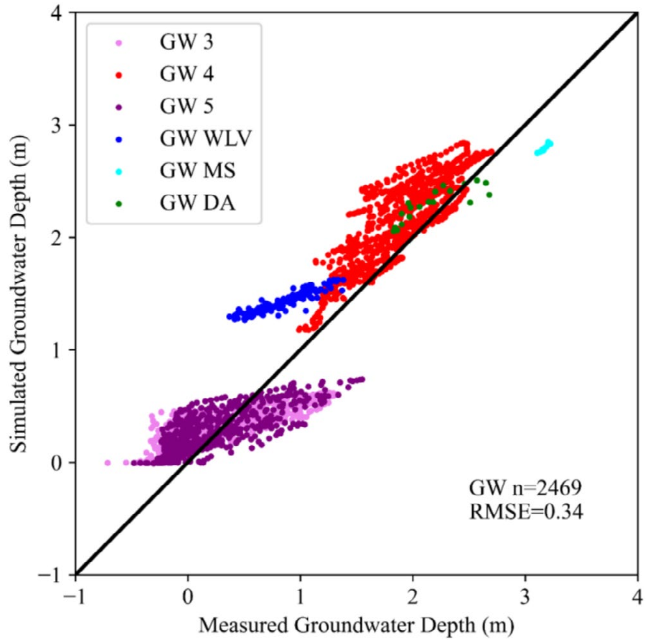

FIGURE 4 | Comparison of measured and simulated groundwater levels at different wells.

4.2 | Groundwater Flow Rate

Modelled groundwater flow velocities in each cell showed that the areas of more intense and rapid water movement areas of faster flow occurred in fluvial and glacial/periglacial deposits, close to the channel network (Figure 6) and peak flow rates could exceed 300 m^3/day. Flow vectors clearly show the spatial pattern of the flow field. These were particularly high in areas of topographic convergence in the upper north-east and central-eastern parts of the catchment. In the upper catchment, equivalent flow rates were very low in the base moraine ($<3 m^3$/day), consistent with the corresponding permeability coefficients. In this part of the catchment, shallow subsurface water was routed rapidly to the channel network via the DRN package. The close proximity of the most rapid groundwater fluxes to the channel network in the mid- and lower catchment corresponds to the area where groundwater–surface water interaction was most sensitive to the seasonal wetting/drying cycles that govern stream flow generation.

4.3 | Groundwater Budgets

When the average annual groundwater budgets for the model domain are examined (Figure 7a), the seasonal patterns of groundwater drawdown and replenishment are clear. Recharge was the highest in the winter when storage intake also peaks. Recharge falls off in the spring and early summer, as evapotranspiration losses increase and storage release increases. Summer storage release accounts for about 40% of the total inflow, whilst the contribution of river recharge was quite low and unaffected by seasonality. Evapotranspiration was the dominant loss from the model domain, accounting for 43%, whilst drain discharge was relatively constant throughout the whole year, though it was the highest in winter. The

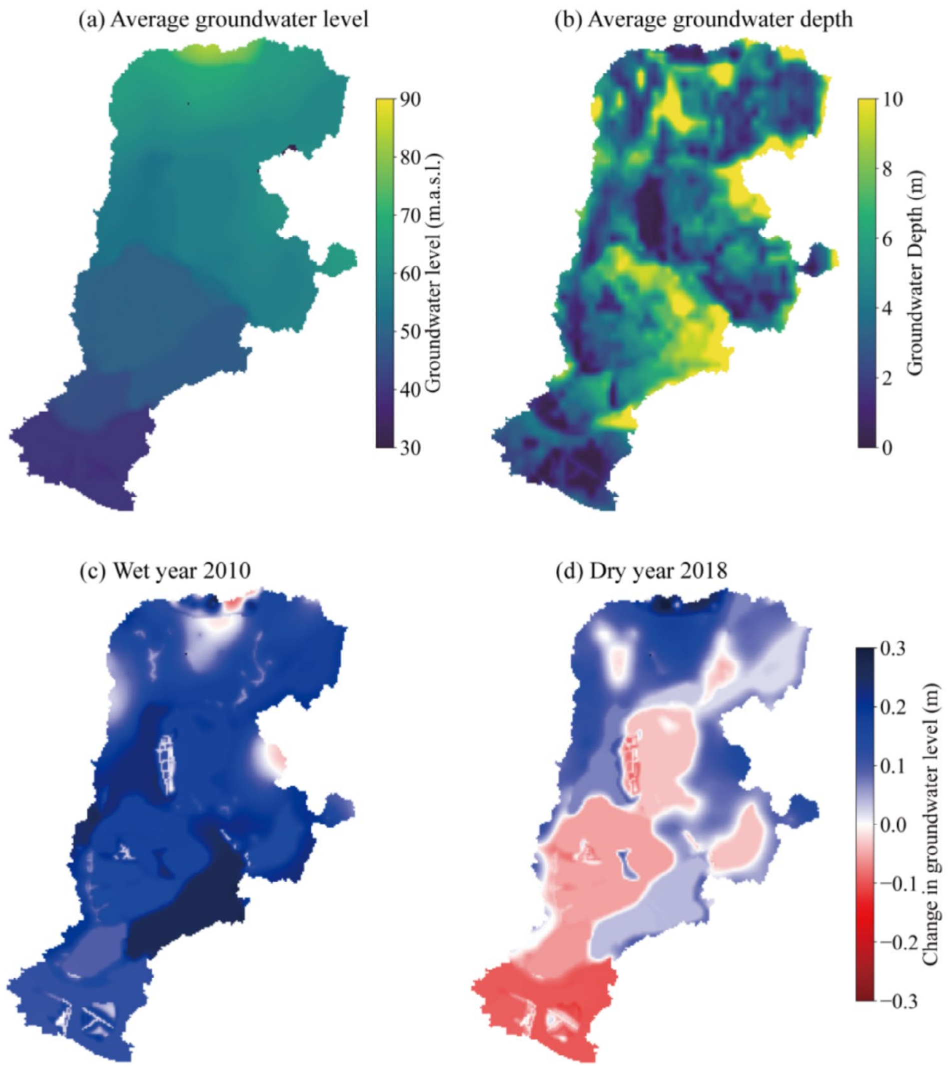

FIGURE 5 | The long-term (2007–2022) average of groundwater elevation and depth, and distribution of differences in wet (2010) and dry (2018) years from the baseline (2007–2022 average water level).

net result of these budgets on the seasonality of groundwater storage changes was very significant (Figure 7b). On average, water surpluses occurred from October of 1 year to February of the next year; during this period, storage increased with groundwater level rising, while deficits begin in March and reach a maximum value (21.5 mm) in June.

The simulated groundwater balance for individual years in DMC showed how strongly variation in recharge was driven by variability in rainfall, which have marked variability as recharge was the largest component of inflow (~76%), followed by storage release (~21%), with river recharge coming in third (Figure 8a). For the whole catchment, the general trend for declining groundwater storage was shown in Figure 8b. Evapotranspiration was generally the dominant source of loss, though river flows can be high in wet years, which also have high storage intake. As a net result of these budget components, between 2007 and 2022, there were only 6 years of water surplus corresponding to positive variations in storage with 9 years of deficits, with the maximum occurring in 2018 and reaching 144 mm (Figure 8b).

4.4 | Groundwater Storage Change

As a result of the water budgets, groundwater storage in the study area showed an overall decreasing trend from 2007 to 2022, with an average decrease of about 2.1 mm each year. The maximum decline over a single calendar year occurred in 2018 with a 20 mm decrease (Figure 9). Spatially, the main changes in groundwater storage are focused in the forested and agricultural areas in the upper and middle catchment, while wetter riparian areas are less affected by increased recharge from rainfall, especially in the central wetlands. This is particularly apparent when comparing the maximum storage change in any given year (Figure 9). The resulting simulations also generally match storage changes calculated from individual groundwater wells (Table 2).

4.5 | Particle Tracking

For the initial 28 particles we input and tracked in the catchment, nine particles were still active at the end of simulation;

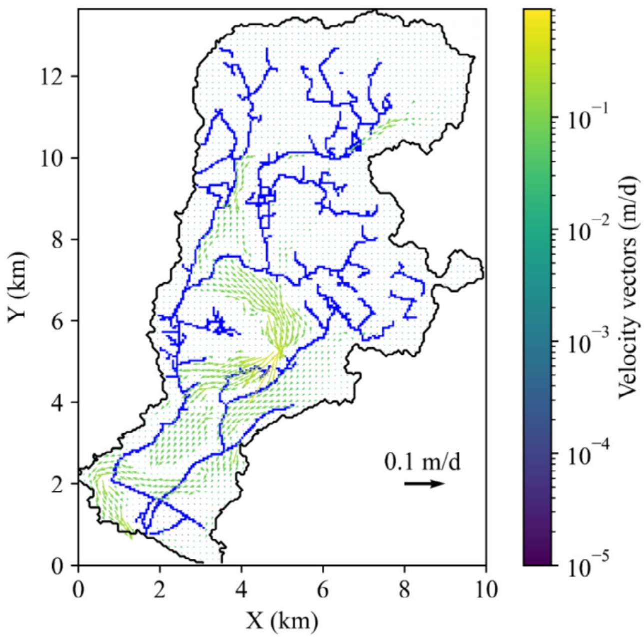

FIGURE 6 | The Groundwater velocity field, velocity vectors indicate the direction and velocity of groundwater flow throughout the model presented as average linear velocity values.

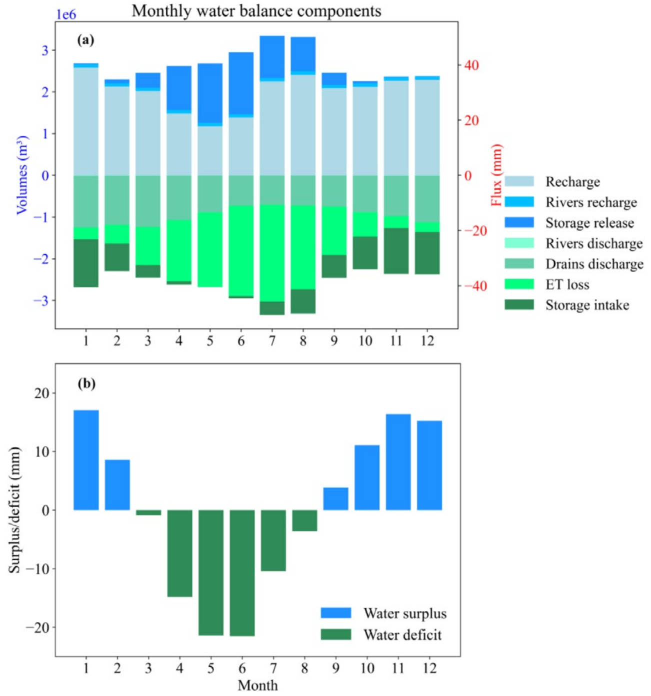

FIGURE 7 | Modelled (a) seasonal groundwater budgets and (b) average monthly water surplus and deficits. Input components: Recharge refers to recharge from precipitation; rivers recharge is the contribution to groundwater from river leakage; storage release is the groundwater sustaining losses. Output components: River discharge is groundwater exfiltration to rivers; drains discharge is groundwater loss to drains; and ET loss is loss from evapotranspiration; storage intake is the replenishment of groundwater.

the remaining particles terminated at the stream network (Figure 10a). Most particles that end in the upper stream network follow a short flow path length originating in the riparian areas. The trajectories of particles with longer flow path lengths were clearly shown in the water flowing from north to south, with geological heterogeneity having an effect. However, spatial interpretation needs to be cautious as this affects projected flow paths, and some of the abrupt changes in particle trajectories may reflect artefacts of the simple model domain, such as the no-flow boundaries and mapped boundaries between geological units. The delineation of the backward flow paths of particles was shown in Figure 10b, which shows that the river water mixed with older water from the surrounding aquifer, and groundwater recharge mainly came from relatively recent precipitation.

The travel time of groundwater from the recharge areas to observation wells (GW DA/4/8/WLV) was generally ~5 years, which is consistent with groundwater age results derived from tritium dating (Figure S6). Yet the river captures a range of variations, including much older water (i.e., decadal), especially in the lower catchment. However, given the importance of drain flow, the model suggests that the stream is likely dominated by younger water.

5 | Discussion

5.1 | Effects of Hydroclimate on the Water Balance and Groundwater Dynamics

Previous studies in the lowland, drought-sensitive DMC have used various hydrological models, calibrated on observational data (Smith, Tetzlaff, Kleine, et al. 2020), to better understand ecohydrological partitioning (Smith et al. 2021), groundwater recharge (Luo et al. 2024b), stream flow generation (Luo et al. 2024a; Wu et al. 2023) and water quality (Wu, Tetzlaff, Yang, et al. 2022). Until the present study, none of this work had used a conventional physically based groundwater model, despite the important role that groundwater has in streamflow generation (Wu, Tetzlaff, Goldhammer, et al. 2022, 2023). The resulting catchment-wide numerical simulations produced by MODFLOW have therefore provided a more comprehensive understanding of the spatio-temporal dynamics of groundwater storage and flow dynamics in DMC, particularly in relation to its interaction with surface waters and sensitivity to hydroclimatic variations.

Using a model calibrated on wells in contrasting, spatially distributed hydrogeological units, we simulated both seasonal and long-term water table dynamics in the shallow groundwater system and changes in the components of the groundwater balance. Because evapotranspiration demands are high relative to rainfall, shallow groundwater and streamflow generation in DMC are highly sensitive to hydroclimatic variations (Figure 2). On a seasonal basis, this generally results in recharge and aquifer replenishment predominating between September and February, with depletion occurring in spring and summer (Figure 7). Over the longer term, rainfall variability is the dominant control on groundwater storage dynamics, with wetter years, like 2010, enabling greater replenishment of storage with 136 mm, but drier years, like 2018, driving depletion of storage. The recent run of

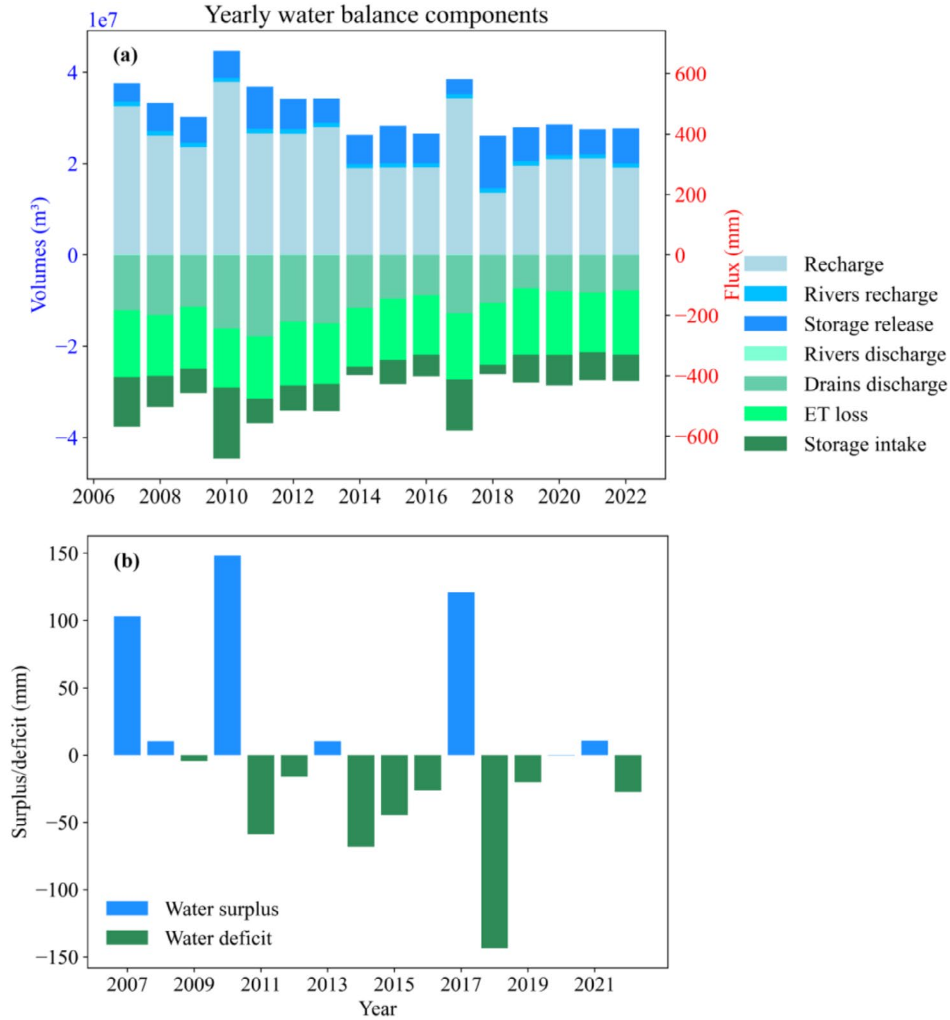

FIGURE 8 | Modelled (a) annual groundwater budgets and (b) average yearly water surplus and deficits. Input components: Recharge refers to recharge from precipitation; rivers recharge is the contribution to groundwater from river leakage; storage release is the groundwater sustaining losses. Output components: River discharge is groundwater exfiltration to rivers; drains discharge is groundwater loss to drains; and ET loss is loss from evapotranspiration; storage intake is the replenishment of groundwater.

dry years since 2018 resulted in a persistent decrease in storage which then accumulates significant groundwater deficits.

In wetter years, the biggest storage changes were modelled for the middle and lower catchment, where larger capacity is available in drier sandier soils underlying forests (Figure 9). Conversely, in drier periods, reductions in storage were more apparent in the arable and wetland soils, where the water table is closer to the surface and evapotranspiration draws down storage disproportionately. This underlines the important influence of land use on groundwater recharge, because of the close link with water use by different vegetation covers. Previous work at DMC has shown how conifer forests, dominated by Scots Pine, have particularly high evapotranspiration rates due to high interception and a longer photosynthetic period for transpiration (Smith, Tetzlaff, Gelbrecht, et al. 2020). However, with a deeper root zone for water uptake and adaptations for stomatal control of transpiration when there is water stress, forests are more resilient to drought than shallower rooting crops, where soil evaporation can also be high (Luo et al. 2024a) (Figure S8). Grasslands occupying the wetter riparian soils have the highest resilience to drought.

5.2 | Effects of Geological Structures and Topographic Features on Spatial–Temporal Patterns of Groundwater–Surface Water Interactions

Spatial patterns of groundwater flow paths and recharge are largely controlled by the distribution and arrangement of contrasting hydrogeologic units in relation to topography (Fan et al. 2023). The main geological structures of the catchment reflect the glacial and periglacial legacy of the last glaciation. However, the DMC lies in the northern part of the much larger depositional environment of the Warsaw–Berlin spillway (Zitzmann 2003). Modelling showed that most of the more rapid catchment groundwater movement is focused on the more permeable glacial/periglacial colluvium and periglacial/fluvial deposits in riparian areas (Figure 6). As these deposits overlay

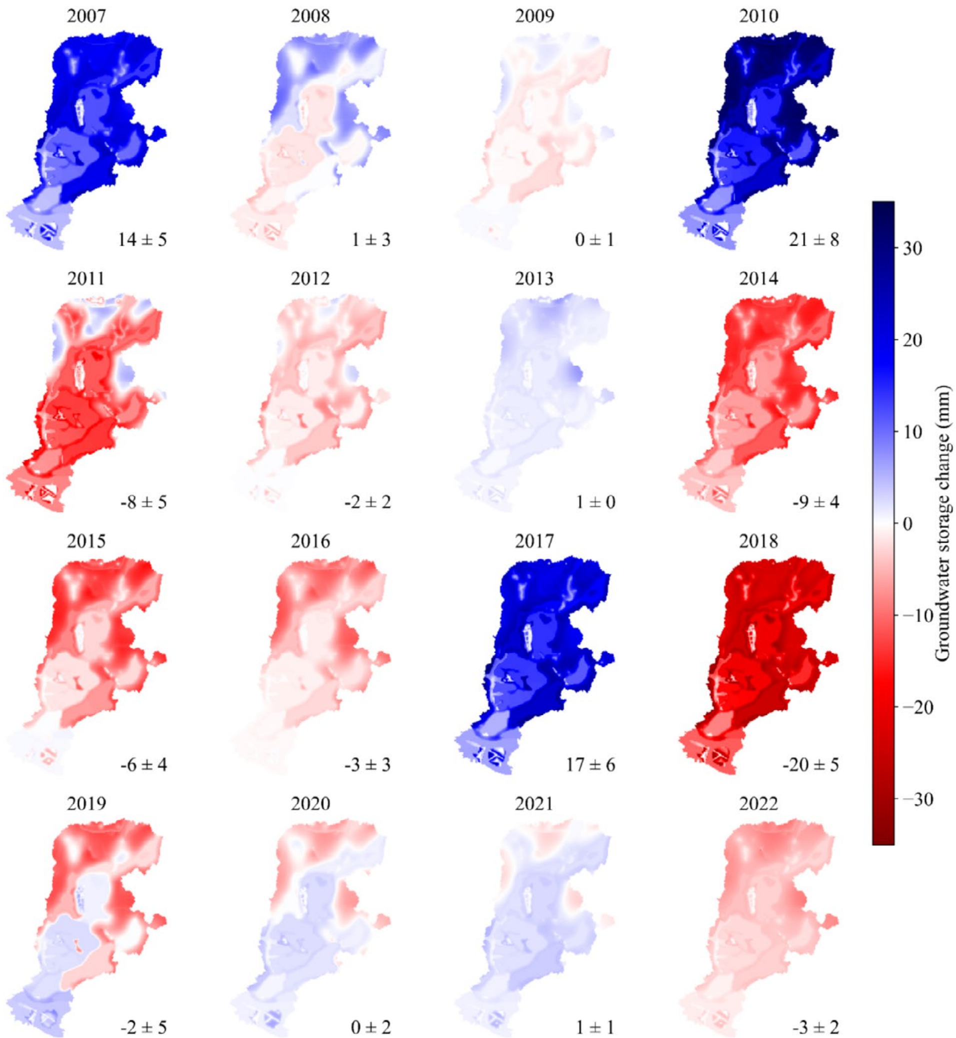

FIGURE 9 | Distribution of differences in long-term (2007–2022) averages of storage change between each year and the baseline. The values shown are average annual change [mm] and standard deviations.

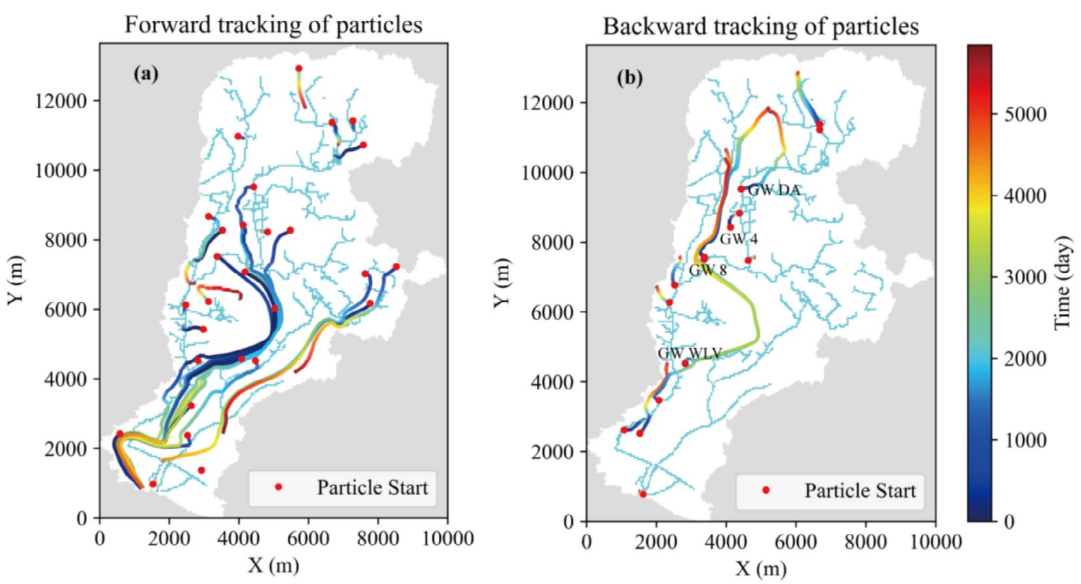

FIGURE 10 | The particle flow paths in the modelled area using (a) forward tracking and (b) backward tracking.

low-permeability clay-dominated ground moraine deposits that impede deeper leakage, they also provide the main conduits for down-valley groundwater flows (Figure 10).

The interaction of the drift distribution, low topography and shallow water table also provides the dominant control on groundwater–surface water interactions and stream flow generation. Close to the stream, valley fluvial deposits were the areas of most intense groundwater–surface water exchange during the winter period when the water table was the highest (Figure 6). These shallow, relatively short flow paths delivered relatively young groundwater to drainage. Both modelled (Figure 10) and tritium-dating (Figure S6) indicate an average age of around ~5 years for the groundwater that provides the main sources of stream flow (Figure S6). This is in line with other isotope-informed ecohydrological modelling studies in the catchment (Smith et al. 2021). The deeper flow paths were longer and mostly controlled by the north–south orientation of the catchment scale topography and alignment of drift deposits. The age of these simulated deeper flow paths was decadal, similar to evidence from tritium samples in the catchment and other groundwater ageing studies elsewhere in Brandenburg (Massmann et al. 2009).

Seasonal streamflow variations were reproduced by the model, though these were generally over-estimated, probably as a result of evapotranspiration being underestimated (Figure S8). Groundwater is the primary control for streamflow generation. Using the DRN package could capture this winter response of increasing runoff. However, because the DRN package allows only for drainage and does not allow for channel infiltration, the spring and summer leakage from the upper channel network (Wang et al. 2025) will be underestimated (McDonald 1988). In the lower catchment where the RIV package was used, there can be reversals of hydraulic gradients as a transmission loss through the streambed can be significant because of the same conductance; however, the boundary conditions in the lower catchment mask this effect by maintaining high water tables (Harbaugh 2005).

5.3 | Spatio-Temporal Patterns of Groundwater Sensitivity to Recovery

In the context of recent increases in the longevity and intensity of droughts in Europe, groundwater is vital to maintaining water supplies and freshwater habitats during periods of negative rainfall anomalies (Imbery et al. 2023). In Germany, groundwater recovery to precipitation following droughts can involve several years of delay, especially in lowland aquifers (Hellwig et al. 2020). The modelling work at DMC showed that the shallow aquifers in the catchment have a high sensitivity to drought. Because of the high evapotranspiration and shallow nature of the groundwater, even in wet years, storage replenishment is limited, and streamflow losses increase (Figure 8). This is consistent with findings from groundwater elsewhere in the North German Plain (Ebeling et al. 2024). However, in a sequence of drier years, such as since 2018, groundwater depletion can become cumulative, though this may have been over-estimated by the model. Because of travel times through the unsaturated zone over much of the catchment, responses of groundwater after drought can be relatively rapid in wet winters (Smith et al. 2022); however, because of ongoing losses to stream flow and evapotranspiration, it will take many years of above-average rainfall to return groundwater levels to those prior to 2018 (Luo et al. 2024b). In this sense, DMC is like other parts of the world where groundwater recharge has been most sensitive to climate changes, especially in areas where potential evapotranspiration exceeds precipitation, and even moderate droughts can substantially reduce groundwater recharge (Berghuijs et al. 2024; Woldeamlak et al. 2007).

Given the hydroclimate and high evapotranspiration losses relative to rainfall, the water balance of DMC is also highly sensitive to land use (Luo et al. 2024a). As shown in Figure S10, the water use of different vegetation impacts groundwater depletion and recovery times. As noted above, tree cover, especially coniferous forests, reduces recharge through high evapotranspiration losses, and the effects of ongoing transpiration under prolonged drought conditions can exacerbate impacts on groundwater storage (Peterson et al. 2021). In the short term, shallow groundwater storage can buffer tree water stress under changing water supply/demand balance where shallow groundwater connections exist, though not indefinitely. When the climate continues to warm, high evapotranspiration continues to deplete groundwater (Condon et al. 2020). Notably, wetland restoration in DMC has raised groundwater levels, which probably increased resistance to drought (Erwin 2009; Wu et al. 2021).

5.4 | Wider Implications

MODFLOW is one of the most commonly used groundwater models and has a wide range of applications in describing groundwater dynamics (Reeve et al. 2001). However, it also has some problems such as uncertainties of parameters at small scales and an effective large-scale nonlinear equations solver (Demissie et al. 2009). In the present study, the geophysical surveys and some basic exploration boreholes helped us to define the flow domain more accurately. In addition, data from boreholes in the catchment characterised groundwater dynamics and aided calibration. However, the simulations still depended on assumptions about the groundwater system, most notable in terms of lateral and lower boundary conditions of the model domain and the hydraulic parameters for the various complex drift deposits, which had to be calibrated (Sun et al. 2022). This results in uncertainty in the modelling results, which can only be viewed as a first approximation and are in need of further development.

Although data-driven groundwater modelling has important practical implications in water management, improvements are needed to aid management at a time when climate change is likely to further reduce the amount and reliability of recharge due to increased variability in rainfall, warmer temperatures and more frequent droughts. A particularly pressing need in cases like DMC is better coupling of ecohydrological models of evapotranspiration under different land covers and groundwater flow models. Of course, this is challenging given that evapotranspiration losses may be derived from root water uptake in both the unsaturated and saturated zones. This limitation would affect other more sophisticated groundwater models, such as

Parflow and Hydrogeosphere, which have great potential for fine simulation of surface groundwater exchange processes (Kollet and Maxwell 2006). However, limited data availability hampers the application of complex models at the regional scale and loosely coupled schemes are more widely applied (Barthel and Banzhaf 2016). The establishment of more refined models to analyse groundwater recharge and groundwater–surface water interactions in drought-sensitive catchments can provide a scientific basis for groundwater management and help alleviate the pressure on water resources due to climate change. In the meantime, current limitations underline the value of ensemble modelling approaches, using different models with contrasting strengths and weaknesses to better understand catchments where water security issues are arising.

6 | Conclusions

Application of MODFLOW to the data-rich DMC catchment provided a preliminary quantitative understanding of spatio-temporal patterns of seasonal and long-term aquifer storage dynamics and groundwater–surface water interactions. It provided a useful framework for integrating data and insights into the function of this drought-sensitive catchment where shallow groundwater provides the main source of stream flow. MODFLOW produced results broadly consistent with other conceptual, ecohydrological and water quality models applied at DMC. It underlined the sensitivity of groundwater recharge to rainfall variations in an environment where evapotranspiration is high. It also further highlights the important influence of vegetation water demands on recharge. However, the modelling also provided new insights into where groundwater flow paths provide the main sources of stream flow and the ages of these younger fluxes, as well as insights into deeper flow paths and their ages through particle tracking. Uncertainties in the modelling mainly stem from unknown boundary conditions around the flow domain and the spatial distribution of hydraulic properties in the diverse glacial and post-glacial drift deposits that dominate the catchment. The study also demonstrated weaknesses in the model structure, particularly in relation to evapotranspiration estimates, as well as the limitations of the DRN package in not allowing channel infiltration. This shows the need for better integration of ecohydrological models and groundwater models. At the same time, this demonstrates the complementarity of ensemble models in catchment studies as learning tools for integrating knowledge and generating competing hypotheses of hydrological function. These in turn can guide future empirical monitoring for hypotheses testing and in order to strengthen future modelling. This remains an imperative to provide a scientific evidence base for integrated land and water management in drought-sensitive lowland catchments.

Acknowledgements

Zhengtao Ying is funded by the Chinese Scholarship Council (CSC). Tetzlaff's contribution was partly funded through the Einstein Research Unit "Climate and Water under Change" from the Einstein Foundation Berlin and Berlin University Alliance (grant no. ERU-2020- 609). Contributions from Soulsby are supported by the Leibnitz Association, German in the project Wetland Restoration in Peatlands and as an International KSLA Guest Professor at SLU by the Wallenberg Foundation (WP2023-0001). Open Access funding enabled and organized by Projekt DEAL.

Data Availability Statement

The data that support the findings of this study are available from the corresponding author upon reasonable request.

References

Adamo, N., N. Al-Ansari, V. Sissakian, J. Laue, and S. Knutsson. 2021. "Geophysical Methods and Their Applications in Dam Safety Monitoring." *Journal of Earth Sciences and Geotechnical Engineering* 11, no. 1: 291–345. https://doi.org/10.47260/jesge/1118.

Ala-aho, P., C. Soulsby, H. Wang, and D. Tetzlaff. 2017. "Integrated Surface-Subsurface Model to Investigate the Role of Groundwater in Headwater Catchment Runoff Generation: A Minimalist Approach to Parameterisation." *Journal of Hydrology* 547: 664–677. https://doi.org/10.1016/j.jhydrol.2017.02.023.

Anderson, M. P., W. W. Woessner, and R. J. Hunt. 2015. *Applied Groundwater Modeling: Simulation of Flow and Advective Transport*. Academic Press.

Bakker, M., V. Post, C. D. Langevin, et al. 2016. "Scripting MODFLOW Model Development Using Python and FloPy." *Groundwater* 54, no. 5: 733–739. https://doi.org/10.1111/gwat.12413.

Barthel, R., and S. Banzhaf. 2016. "Groundwater and Surface Water Interaction at the Regional-Scale–A Review With Focus on Regional Integrated Models." *Water Resources Management* 30, no. 1: 1–32.

Berghuijs, W. R., R. A. Collenteur, S. Jasechko, et al. 2024. "Groundwater Recharge Is Sensitive to Changing Long-Term Aridity." *Nature Climate Change* 14, no. 4: 357–363. https://doi.org/10.1038/s41558-024-01953-z.

Bianchi, M., J. Scheidegger, A. Hughes, et al. 2024. "Simulation of National-Scale Groundwater Dynamics in Geologically Complex Aquifer Systems: An Example From Great Britain." *Hydrological Sciences Journal* 69, no. 5: 572–591. https://doi.org/10.1080/02626667.2024.2320847.

Condon, L. E., A. L. Atchley, and R. M. Maxwell. 2020. "Evapotranspiration Depletes Groundwater Under Warming Over the Contiguous United States." *Nature Communications* 11, no. 1: 873. https://doi.org/10.1038/s41467-020-14688-0.

Dehghanipour, A. H., B. Zahabiyoun, G. Schoups, and H. Babazadeh. 2019. "A WEAP-MODFLOW Surface Water-Groundwater Model for the Irrigated Miyandoab Plain, Urmia Lake Basin, Iran: Multi-Objective Calibration and Quantification of Historical Drought Impacts." *Agricultural Water Management* 223: 105704. https://doi.org/10.1016/j.agwat.2019.105704.

Demissie, Y. K., A. J. Valocchi, B. S. Minsker, and B. A. Bailey. 2009. "Integrating a Calibrated Groundwater Flow Model With Error-Correcting Data-Driven Models to Improve Predictions." *Journal of Hydrology* 364, no. 3–4: 257–271. https://doi.org/10.1016/j.jhydrol.2008.11.007.

Devia, G. K., B. P. Ganasri, and G. S. Dwarakish. 2015. "A Review on Hydrological Models." *Aquatic Procedia* 4: 1001–1007. https://doi.org/10.1016/j.aqpro.2015.02.126.

Doherty, J. 2020. "A Simple Lumped Parameter Model for Unsaturated Zone Processes. Watermark Numerical Computing, Brisbane, Australia."

Döll, P., H. Hoffmann-Dobrev, F. T. Portmann, et al. 2012. "Impact of Water Withdrawals From Groundwater and Surface Water on Continental Water Storage Variations." *Journal of Geodynamics* 59-60: 143–156. https://doi.org/10.1016/j.jog.2011.05.001.

Ebeling, P., A. Musolff, R. Kumar, A. Hartmann, and J. H. Fleckenstein. 2024. "Groundwater Head Responses to Droughts Across Germany." *EGUsphere* 2024: 1–37. https://doi.org/10.5194/egusphere-2024-2761.

Erwin, K. L. 2009. "Wetlands and Global Climate Change: The Role of Wetland Restoration in a Changing World." *Wetlands Ecology and Management* 17, no. 1: 71–84. https://doi.org/10.1007/s11273-008-9119-1.

Fan, X., T. J. Peterson, B. J. Henley, and M. Arora. 2023. "Groundwater Sensitivity to Climate Variations Across Australia." *Water Resources Research* 59, no. 11: e2023WR035036. https://doi.org/10.1029/2023WR035036.

Fetter, C. W. 2018. *Applied Hydrogeology*. Waveland Press.

Freeze, R. A., and J. A. Cherry. 1979. "Groundwater Prentice-Hall." *Englewood Cliffs, NJ* 176: 161–177.

Frei, S., J. Fleckenstein, S. Kollet, and R. M. Maxwell. 2009. "Patterns and Dynamics of River–Aquifer Exchange With Variably-Saturated Flow Using a Fully-Coupled Model." *Journal of Hydrology* 375, no. 3–4: 383–393. https://doi.org/10.1016/j.jHydrol.2009.06.038.

Gelbrecht, J., H. Lengsfeld, R. Pöthig, and D. Opitz. 2005. "Temporal and Spatial Variation of Phosphorus Input, Retention and Loss in a Small Catchment of NE Germany." *Journal of Hydrology* 304, no. 1–4: 151–165. https://doi.org/10.1016/j.jhydrol.2004.07.028.

Goderniaux, P., S. Brouyère, H. J. Fowler, et al. 2009. "Large Scale Surface–Subsurface Hydrological Model to Assess Climate Change Impacts on Groundwater Reserves." *Journal of Hydrology* 373, no. 122: 138. https://doi.org/10.1016/j.jHydrol.2009.04.017.

Harbaugh, A. W. 2005. "MODFLOW-2005, the US Geological Survey Modular Ground-Water Model: The Ground-Water Flow Process, 6. US Department of the Interior, US Geological Survey Reston, VA, USA."

Hellwig, J., I. de Graaf, M. Weiler, and K. Stahl. 2020. "Large-Scale Assessment of Delayed Groundwater Responses to Drought." *Water Resources Research* 56, no. 2: e2019WR025441. https://doi.org/10.1029/2019WR025441.

Imbery, F., K. Friedrich, R. Fleckenstein, et al. 2023. "Klimatologischer Rückblick auf 2022: Das Sonnenscheinreichste Und Eines Der Beiden Wärmsten Jahre in Deutschland. DWD." https://www.dwd.de/DE/klimaumwelt/aktuelle_meldungen/230123/artikel_jahresrueckblick-2022.html.

Jasechko, S., H. Seybold, D. Perrone, et al. 2024. "Rapid Groundwater Decline and Some Cases of Recovery in Aquifers Globally." *Nature* 625, no. 7996: 715–721. https://doi.org/10.1038/s41586-023-06879-8.

Kleine, L., D. Tetzlaff, A. Smith, M. Dubbert, and C. Soulsby. 2021. "Modelling Ecohydrological Feedbacks in Forest and Grassland Plots Under a Prolonged Drought Anomaly in Central Europe 2018–2020." *Hydrological Processes* 35, no. 8: e14325. https://doi.org/10.1002/hyp.14325.

Kleine, L., D. Tetzlaff, A. Smith, T. Goldhammer, and C. Soulsby. 2021. "Using Isotopes to Understand Landscape-Scale Connectivity in a Groundwater-Dominated, Lowland Catchment Under Drought Conditions." *Hydrological Processes* 35, no. 5: e14197. https://doi.org/10.1002/hyp.14197.

Kløve, B., P. Ala-Aho, G. Bertrand, et al. 2014. "Climate Change Impacts on Groundwater and Dependent Ecosystems." *Journal of Hydrology* 518: 250–266. https://doi.org/10.1016/j.jhydrol.2013.06.037.

Kollet, S. J., and R. M. Maxwell. 2006. "Integrated Surface–Groundwater Flow Modeling: A Free-Surface Overland Flow Boundary Condition in a Parallel Groundwater Flow Model." *Advances in Water Resources* 29, no. 7: 945–958.

Kottek, M., J. Grieser, C. Beck, B. Rudolf, and F. Rubel. 2006. "World Map of the Köppen-Geiger Climate Classification Updated." *Meteorologische Zeitschrift* 15: 259–263. https://doi.org/10.1127/0941-2948/2006/013.

Luo, S., D. Tetzlaff, A. Smith, and C. Soulsby. 2024a. "Assessing Impacts of Alternative Land Use Strategies on Water Partitioning, Storage and Ages in Drought-Sensitive Lowland Catchments Using Tracer-Aided Ecohydrological Modelling." *Hydrological Processes* 38, no. 4: e15126. https://doi.org/10.1002/hyp.15126.

Luo, S., D. Tetzlaff, A. Smith, and C. Soulsby. 2024b. "Long-Term Drought Effects on Landscape Water Storage and Recovery Under Contrasting Landuses." *Journal of Hydrology* 636: 131339. https://doi.org/10.1016/j.jhydrol.2024.131339.

Ma, R., K. Chen, C. B. Andrews, et al. 2024. "Methods for Quantifying Interactions Between Groundwater and Surface Water." *Annual Review of Environment and Resources* 49: 623–653. https://doi.org/10.1146/annurev-environ-111522-104534.

Massmann, G., J. Sültenfuß, and A. Pekdeger. 2009. "Analysis of Long-Term Dispersion in a River-Recharged Aquifer Using Tritium/Helium Data." *Water Resources Research* 45, no. 2: 6746. https://doi.org/10.1029/2007WR006746.

McDonald, M. 1988. *A Modular Three-Dimensional Finite-Difference Ground-Water Flow Model*. Techniques of Water-Resources Investigations of the United States Geological Survey.

Ntona, M. M., G. Busico, M. Mastrocicco, and N. Kazakis. 2022. "Modeling Groundwater and Surface Water Interaction: An Overview of Current Status and Future Challenges." *Science of the Total Environment* 846: 157355. https://doi.org/10.1016/j.scitotenv.2022.157355.

Oiro, S., J.-C. Comte, C. Soulsby, A. MacDonald, and C. Mwakamba. 2020. "Depletion of Groundwater Resources Under Rapid Urbanisation in Africa: Recent and Future Trends in the Nairobi Aquifer System, Kenya." *Hydrogeology Journal* 28: 2635–2656. https://doi.org/10.1007/s10040-020-02236-5.

Panagopoulos, G. 2012. "Application of MODFLOW for Simulating Groundwater Flow in the Trifilia Karst Aquifer, Greece." *Environmental Earth Sciences* 67, no. 7: 1877–1889. https://doi.org/10.1007/s12665-012-1630-2.

Peterson, T. J., M. Saft, M. Peel, and A. John. 2021. "Watersheds May Not Recover From Drought." *Science* 372, no. 6543: 745–749. https://doi.org/10.1126/science.abd508.

Reeve, A., J. Warzocha, P. Glaser, and D. Siegel. 2001. "Regional Ground-Water Flow Modeling of the Glacial Lake Agassiz Peatlands, Minnesota." *Journal of Hydrology* 243, no. 1–2: 91–100. https://doi.org/10.1016/S0022-1694(00)00402-9.

Richey, A. S., B. F. Thomas, M. H. Lo, et al. 2015. "Quantifying Renewable Groundwater Stress With GRACE." *Water Resources Research* 51, no. 7: 5217–5238. https://doi.org/10.1002/2015WR017349.

Saha, G. C., J. Li, R. W. Thring, F. Hirshfield, and S. S. Paul. 2017. "Temporal Dynamics of Groundwater-Surface Water Interaction Under the Effects of Climate Change: A Case Study in the Kiskatinaw River Watershed, Canada." *Journal of Hydrology* 551: 440–452. https://doi.org/10.1016/j.jhydrol.2017.06.008.

Santos, R., L. S. Fernandes, J. Moura, M. Pereira, and F. Pacheco. 2014. "The Impact of Climate Change, Human Interference, Scale and Modeling Uncertainties on the Estimation of Aquifer Properties and River Flow Components." *Journal of Hydrology* 519: 1297–1314. https://doi.org/10.1016/j.jHydrol.2014.09.001.

Smith, A., D. Tetzlaff, J. Gelbrecht, L. Kleine, and C. Soulsby. 2020. "Riparian Wetland Rehabilitation and Beaver Re-Colonization Impacts on Hydrological Processes and Water Quality in a Lowland Agricultural Catchment." *Science of the Total Environment* 699: 134302. https://doi.org/10.1016/j.scitotenv.2019.134302.

Smith, A., D. Tetzlaff, L. Kleine, M. Maneta, and C. Soulsby. 2021. "Quantifying the Effects of Land Use and Model Scale on Water Partitioning and Water Ages Using Tracer-Aided Ecohydrological Models." *Hydrology and Earth System Sciences* 25, no. 4: 2239–2259. https://doi.org/10.5194/hess-25-2239-2021.

Smith, A., D. Tetzlaff, L. Kleine, M. P. Maneta, and C. Soulsby. 2020. "Isotope-Aided Modelling of Ecohydrologic Fluxes and Water Ages Under Mixed Land Use in Central Europe: The 2018 Drought and Its Recovery." *Hydrological Processes* 34, no. 16: 3406–3425. https://doi.org/10.1002/hyp.13838.

Smith, A., D. Tetzlaff, M. Maneta, and C. Soulsby. 2022. "Critical Zone Response Times and Water Age Relationships Under Variable Catchment Wetness States: Insights Using a Tracer-Aided Ecohydrological Model." *Water Resources Research* 58, no. 4: e2021WR030584. https://doi.org/10.1029/2021WR030584.

Soulsby, C., C. Birkel, J. Geris, J. Dick, C. Tunaley, and D. Tetzlaff. 2015. "Stream Water Age Distributions Controlled by Storage Dynamics and Nonlinear Hydrologic Connectivity: Modeling With High-Resolution Isotope Data." *Water Resources Research* 51, no. 9: 7759–7776. https://doi.org/10.1002/2015WR017888.

Sun, J., L. Hu, D. Li, K. Sun, and Z. Yang. 2022. "Data-Driven Models for Accurate Groundwater Level Prediction and Their Practical Significance in Groundwater Management." *Journal of Hydrology* 608: 127630. https://doi.org/10.1016/j.jhydrol.2022.127630.

Taylor, R. G., B. Scanlon, P. Döll, et al. 2013. "Ground Water and Climate Change." *Nature Climate Change* 3, no. 4: 322–329. https://doi.org/10.1038/nclimate1744.

Tetzlaff, D., H. Laudon, S. Luo, and C. Soulsby. 2024. "Ecohydrological Resilience and the Landscape Water Storage Continuum in Droughts." *Nature Water* 2, no. 10: 1–4. https://doi.org/10.1038/s44221-024-00300-y.

Tetzlaff, D., A. Smith, L. Kleine, H. Daempfling, J. Freymueller, and C. Soulsby. 2022. "Integrated Ecohydrological Hydrometric and Stable Water Isotope Data of a Drought-Sensitive Mixed Land Use Lowland Catchment." *Earth System Science Data Discussions* 15, no. 4: 1–19. https://doi.org/10.5194/essd-15-1543-2023.

Tian, Y., Y. Zheng, B. Wu, X. Wu, J. Liu, and C. Zheng. 2015. "Modeling Surface Water-Groundwater Interaction in Arid and Semi-Arid Regions With Intensive Agriculture." *Environmental Modelling and Software* 63: 170–184. https://doi.org/10.1016/j.envsoft.2014.10.011.

Wang, F., D. Tetzlaff, T. Goldhammer, J. Freymueller, and C. Soulsby. 2025. "Hydrological Connectivity Drives Intra-And Inter-Annual Variation in Water Quality in an Intermittent Stream Network in a Mixed Land Use Catchment Under Drought." *Journal of Hydrology* 648: 132420. https://doi.org/10.1016/j.jhydrol.2024.132420.

Winter, T. C. 1999. "Relation of Streams, Lakes, and Wetlands to Groundwater Flow Systems." *Hydrogeology Journal* 7, no. 1: 28–45. https://doi.org/10.1007/s100400050178.

Woldeamlak, S. T., O. Batelaan, and F. De Smedt. 2007. "Effects of Climate Change on the Groundwater System in the Grote-Nete Catchment, Belgium." *Hydrogeology Journal* 15: 891–901.

Wu, S., D. Tetzlaff, T. Goldhammer, J. Freymueller, and C. Soulsby. 2022. "Tracer-Aided Identification of Hydrological and Biogeochemical Controls on In-Stream Water Quality in a Riparian Wetland." *Water Research* 222: 118860. https://doi.org/10.1016/j.watres.2022.118860.

Wu, S., D. Tetzlaff, T. Goldhammer, and C. Soulsby. 2021. "Hydroclimatic Variability and Riparian Wetland Restoration Control the Hydrology and Nutrient Fluxes in a Lowland Agricultural Catchment." *Journal of Hydrology* 603: 126904. https://doi.org/10.1016/j.jhydrol.2021.126904.

Wu, S., D. Tetzlaff, X. Yang, A. Smith, and C. Soulsby. 2023. "Integrating Tracers and Soft Data Into Multi-Criteria Calibration: Implications From Distributed Modeling in a Riparian Wetland." *Water Resources Research* 59, no. 11: e2023WR035509. https://doi.org/10.1029/2023WR035509.

Wu, S., D. Tetzlaff, X. Yang, and C. Soulsby. 2022. "Disentangling the Influence of Landscape Characteristics, Hydroclimatic Variability and Land Management on Surface Water NO3-N Dynamics: Spatially Distributed Modeling Over 30 Yr in a Lowland Mixed Land Use Catchment." *Water Resources Research* 58, no. 2: e2021WR030566. https://doi.org/10.1029/2021WR030566.

Yang, C., L. E. Condon, and R. M. Maxwell. 2025. "Unravelling Groundwater–Stream Connections Over the Continental United States." *Nature Water* 3: 70–79. https://doi.org/10.1038/s44221-024-00366-8.

Ying, Z., D. Tetzlaff, J. Freymueller, et al. 2024. "Developing a Conceptual Model of Groundwater–Surface Water Interactions in a Drought Sensitive Lowland Catchment Using Multi-Proxy Data." *Journal of Hydrology* 628: 130550. https://doi.org/10.1016/j.jhydrol.2023.130550.

Yuan, X., Y. Wang, P. Ji, P. Wu, J. Sheffield, and J. A. Otkin. 2023. "A Global Transition to Flash Droughts Under Climate Change." *Science* 380, no. 6641: 187–191. https://doi.org/10.1126/science.abn6301.

Zipper, S. C., T. Gleeson, Q. Li, and B. Kerr. 2021. "Comparing Streamflow Depletion Estimation Approaches in a Heavily Stressed, Conjunctively Managed Aquifer." *Water Resources Research* 57, no. 2: 17. https://doi.org/10.1029/2020wr027591.

Zitzmann, A. 2003. "Die Geologische Übersichtskarte 1: 200 000–von der Karte bis zur Sachdatenbank." *Zeitschrift der Deutschen Geologischen Gesellschaft* 154, no. 1: 121–139. https://doi.org/10.1127/zdgg/154/2003/121.

Supporting Information

Additional supporting information can be found online in the Supporting Information section.